

Available online at [www.sciencedirect.com](http://www.sciencedirect.com)

ScienceDirect

journal homepage: [www.e-jmii.com](http://www.e-jmii.com)

Original Article

# RAGE participates in the intracellular transport of *Campylobacter jejuni* cytolethal distending toxin

Yu-Fang Chang<sup>a,2,1</sup>, Yi-Ping Huang<sup>b,1</sup>, Chia-Huei Chou<sup>c</sup>,  
Mao-Wang Ho<sup>c</sup>, Hwai-Jeng Lin<sup>d,e</sup>, Chun-Ya Chen<sup>f</sup>, Hui-Yu Wu<sup>a</sup>,  
Yi-Ru Lai<sup>a</sup>, Yuan-Haw Lee<sup>a</sup>, Cheng-Hsun Chiu<sup>a,g</sup>,  
Chih-Ho Lai<sup>a,g,h,i,j,\*</sup>



<sup>a</sup> Graduate Institute of Biomedical Sciences, Department of Microbiology and Immunology, Chang Gung University, Taoyuan, Taiwan

<sup>b</sup> Department of Physiology, School of Medicine, China Medical University, Taichung, Taiwan

<sup>c</sup> Departments of Infectious Disease, School of Medicine, China Medical University and Hospital, Taichung, Taiwan

<sup>d</sup> Division of Gastroenterology and Hepatology, Department of Internal Medicine, Shuang-Ho Hospital, New Taipei, Taiwan

<sup>e</sup> Division of Gastroenterology and Hepatology, Department of Internal Medicine, School of Medicine, College of Medicine, Taipei Medical University, Taipei, Taiwan

<sup>f</sup> Department of Laboratory Medicine, Taichung Veterans General Hospital Chiayi Branch, Chiayi, Taiwan

<sup>g</sup> Molecular Infectious Disease Research Center, Department of Pediatrics, Chang Gung Memorial Hospital, Linkou, Taiwan

<sup>h</sup> Department of Microbiology and Immunology, School of Medicine, China Medical University, Taichung, Taiwan

<sup>i</sup> Department of Nursing, Asia University, Taichung, Taiwan

<sup>j</sup> Research Center for Emerging Viral Infections, Chang Gung University, Taoyuan, Taiwan

Received 24 November 2023; received in revised form 6 June 2024; accepted 8 July 2024  
Available online 3 August 2024

## KEYWORDS

*Campylobacter jejuni*;  
Cytolethal distending

**Abstract** *Background:* Cytolethal distending toxin (CDT) belongs to the genotoxin family and is closely related to *Campylobacter jejuni*-associated gastroenteritis. We recently reported that CDT triggers the danger-associated molecular pattern (DAMP) signaling to exert deleterious effects on host cells. However, how CDT traffics in cells and the mechanism of CDT intoxication remain to be elucidated.

\* Corresponding author. Department of Microbiology and Immunology, Chang Gung University, Taiwan.

E-mail address: [chlai@mail.cgu.edu.tw](mailto:chlai@mail.cgu.edu.tw) (C.-H. Lai).

<sup>1</sup> Equal contribution to this work.

<sup>2</sup> The author's current affiliation: Department of Laboratory Medicine, Chang Gung Memorial Hospital, Linkou, Taiwan.

toxin;  
Intracellular  
transport

**Methods:** Recombinant CDT subunits (CdtA, CdtB, and CdtC) were purified, and their activity was characterized in gastrointestinal cells. Molecular approaches and image tracking were employed to analyze the delivery of CDT in host cells.

**Results:** In this study, we found that CDT interacts with the receptor of advanced glycation end products (RAGE) and high mobility group box 1 (HMGB1) to enter the cells. Our results further showed that CdtB transport in cells through the dynamin-dependent endocytic pathway and lysosome is involved in this process. Conversely, blockage of RAGE signaling resulted in a reduction in CDT-arrested cell cycles, indicating that RAGE is involved in CDT intracellular transport and its subsequent pathogenesis.

**Conclusion:** Our results demonstrate that RAGE is important for CDT trafficking in the cells. These findings expand our understanding of important issues related to host cell intoxication by *C. jejuni* CDT.

Copyright © 2024, Taiwan Society of Microbiology. Published by Elsevier Taiwan LLC. This is an open access article under the CC BY-NC-ND license (<http://creativecommons.org/licenses/by-nc-nd/4.0/>).

## Introduction

*Campylobacter jejuni* is the predominant causative agent of human gastroenteritis globally.<sup>1,2</sup> While the disease typically manifests as mild in healthy adults, it can lead to severe and prolonged symptoms in young children, elderly individuals, and those with compromised immune systems.<sup>3,4</sup> Among the virulence factors presented in *C. jejuni*, cytolethal distending toxin (CDT) has been discerned as playing a pivotal role in the pathogenicity induced by *C. jejuni*.<sup>5,6</sup>

CDT is a bacterial genotoxin known for inducing DNA damage in host cells,<sup>7</sup> and the genotoxin exhibited in several Gram-negative bacteria, such as *Aggregatibacter actinomycetemcomitans*, *C. jejuni*, *Escherichia coli*, and *Haemophilus ducreyi*.<sup>8</sup> As an AB<sub>2</sub> toxin, CDT is composed of one active subunit (CdtB), and two binding subunits (CdtA and CdtC).<sup>9</sup> In our earlier work, we demonstrated that both CdtA and CdtC bind to lipid rafts on the cytoplasmic membrane, facilitating the delivery of CdtB into host cells through the endocytic pathway.<sup>10</sup> It is believed that CdtB, as a DNase, translocates into the nucleus, where it induces double-strand breaks (DSBs) and subsequently arrests the cell cycle at the G2/M phase.<sup>9</sup>

While the specific receptor for CDT binding has not yet been identified, and discordant results have been reported,<sup>11</sup> it is widely recognized that the interaction between CDT and lipid rafts involves a collaborative effort between CdtA and CdtC, forming together a deep groove to adhere to the cell surface.<sup>12</sup> In a previous study using PhITSeq to examine whether CDTs from different bacterial origins employ unique pathways for cellular entry and intoxication, it was discovered that TMEM127, GPR107, and TM9SF4, all of which are cell membrane proteins, appear to play pivotal roles in facilitating the trafficking of *C. jejuni* CDT.<sup>13</sup> Following endocytosis, the translocation of CDT to the nucleus has predominantly been attributed to retrograde transport through the Golgi apparatus and endoplasmic reticulum (ER).<sup>14</sup> The intricate molecular mechanisms governing the subsequent transport from ER to the nucleus remain largely unknown. Since there is presently no empirical evidence supporting the presence of a nuclear localization signal (NLS) in CdtB of *C. jejuni*, a

previous study has proposed the potential involvement of ER-associated degradation (ERAD) pathway in mediating CDT trafficking to the nucleus.<sup>15</sup> Nevertheless, the findings of this study indicated that *C. jejuni*-CDT exhibits the least dependency on, even no requirement for, several key factors within the ERAD pathway. Therefore, we posit that *C. jejuni*-CDT has evolved a unique strategy for nucleus trafficking.

As delineated in our previous study, CDT elicits inflammatory response by upregulating the expression of high mobility group box 1 (HMGB1) and the receptor for advanced glycation end products (RAGE).<sup>16</sup> HMGB1 is an evolutionarily highly conserved nuclear non-histone DNA-binding protein.<sup>17</sup> Within the nucleus, HMGB1 participates in genome organization, DNA replication, and DNA repair.<sup>18</sup> When HMGB1 is actively transported or passively released into the extracellular milieu, it functions as a danger-associated molecular pattern (DAMP).<sup>19</sup> RAGE, on the other hand, is a multiligand pattern recognition receptor (PRR) expressed ubiquitously across various cell types. Its interaction with HMGB1 has frequently been reported to be associated with inflammatory diseases.<sup>20</sup> However, the detailed mechanism of CDT delivery into the cells warrants further investigation. Here, we present that CDT is transported within cells through the interaction between HMGB1 and RAGE, and the inhibition of RAGE leads to a reduction in the cytopathic effects induced by CDT.

## Materials and methods

### Cell culture

AGS cells (ATCC CRL-1739, a gastrointestinal-derived epithelial cell line), were cultured in F12 medium (HyClone) containing 10% fetal bovine serum. The cells were cultured at 37 °C in a humid atmosphere with 5% CO<sub>2</sub>.

### Preparation of recombinant *C. jejuni* CDT

Each recombinant His-tagged CDT subunit was prepared following the previous study.<sup>10</sup> Briefly, *E. coli* BL21 (DE3) harboring *cdtA*, *cdtB*, and *cdtC* expression plasmids were

cultured in LB broth with ampicillin (100 µg/ml) at 37 °C. Isopropyl-β-D-thiogalactopyranoside (1 M) was used to induce the expression of each recombinant protein. Both *cdtA*- and *cdtB*-bearing *E. coli* were incubated at 37 °C for 5 h, whereas *E. coli*-containing *cdtC* was incubated at 16 °C for 20 h. Bacteria were collected by centrifugation at 7500 rpm at 4 °C for 5 min, and the pellet was treated with lysis buffer. After sonicating for 15 min, bacterial lysate was purified by metal affinity chromatography (Clontech). Each recombinant CDT was assessed by SDS-PAGE and Western blot assay (Fig. S1). Antibodies against each CDT subunit were generated as previously described.<sup>10</sup> Each recombinant CDT subunit (200 nM) was added to cell culture medium and incubated at 37 °C for 30 min to reconstitute a CDT holotoxin. CDT activity was then verified using flow cytometric analysis, showing marked cell distension and cell cycle arrest at G2/M after 24 h of CDT holotoxin exposure (Fig. S2).

### Cell cycle analysis

AGS cells were mock-treated (CDT untreated) or treated with 100 nM CDT holotoxin for 0, 24, 48, and 72 h. After PBS washing, cells were fixed in ice-cold 70% ethanol. Cells were stained with 20 µg/ml propidium iodide (Sigma-Aldrich) for 1 h on ice. Cell cycle analysis was performed using FACScalibur flow cytometry (Becton Dickinson).

### Co-immunoprecipitation (Co-IP) assay

Co-IP assay was conducted with Dynabeads Protein G following the manufacturer's instructions (Thermo Fisher Scientific).<sup>16</sup> CDT holotoxin (100 nM) was added to the cells and incubated for 12 h. Cell lysates were prepared and incubated with Dynabeads Protein G (magnetic beads are at 30 mg/ml in PBS (pH 7.4) with 0.01% Tween-20) for immunoprecipitation. The anti-RAGE antibody or control isotype anti-IgG was added to create the co-IP complex. The proteins of interest were eluted and analyzed by Western blot assay. The membranes were probed with the primary antibodies against RAGE, CdtB, and β-actin, respectively.

### Immunofluorescence staining

AGS cells were seeded on coverslips and cultured overnight, then exposed to CDT holotoxin (100 nM) for 6 h. The cells were fixed with 4% paraformaldehyde for 30 min and permeabilized by 0.1% Triton X-100 for 30 min. To analyze CdtB localization in the cytoplasmic compartments, cells were incubated with an anti-CdtB antibody,<sup>10</sup> and then stained with Alexa Fluor 488-conjugate anti-mouse IgG (Jackson ImmunoResearch Laboratories). Lysosome was stained with anti-LAMP1 Alexa Fluor 647 conjugate antibody (Abcam), and cathepsin D was probed by anti-cathepsin D antibody (Abcam). Nuclei were stained with Hoechst 33342 for 30 min and the cell membrane was probed with cholera toxin subunit B (CTx-B-Alexa Fluor 555 conjugated). The stained cells were observed under a confocal laser scanning microscope (LSM780, Carl Zeiss).

### Preparation of cytoplasmic and nuclear fractions

Cells were pretreated with 100 µM dynasore (Sigma-Aldrich), and then exposed to 100 nM CDT holotoxin for 90 min. The extraction of cytoplasmic and nuclear proteins was conducted by using the Minute Cytoplasmic and Nuclear Extraction Kit (Invent Biotechnologies). Briefly, after cell harvesting, cytoplasmic extraction buffer was added to the cell pellet, followed by vortexing for 15 s. The mixture was then centrifuged at 14,000×g for 5 min at 4 °C, resulting in the isolation of the supernatant as the cytoplasmic extract. Subsequently, the pellet was treated with nuclear extraction buffer, vortexed for 15 s, and subjected to centrifugation at 14,000×g for 30 s at 4 °C to isolate the nuclear fraction. Finally, both cytoplasmic and nuclear fractions of the cell lysates were analyzed by Western blot assay.

### SDS-PAGE analysis and Western blot assay

AGS cells were pretreated with 100 µM dynasore, and then incubated with each recombinant CDT protein for 90 min. Cell lysates were resolved by SDS-PAGE and transferred onto polyvinylidene difluoride membranes (Millipore). The membranes were incubated with primary antibodies against LAMP1, EEA1, RAB7, RAGE, and β-actin, respectively, at 4 °C overnight with gentle shaking. The membranes were then incubated with horseradish peroxidase-conjugated secondary antibody (Millipore) for 1 h at room temperature. The proteins of interest were detected by ECL Western Blotting Detection Reagents (GE Healthcare) and visualized using Azure c400 system with AzureSpot Analysis Software (Azure Biosystems).<sup>21</sup>

### Knockout of RAGE

RAGE-knockout (RAGE-KO) was conducted by using the CRISPR-Cas system (Dharmacon, Lafayette, CO, USA). The single guide RNA (sgRNA) targeted DNA sequence is 5'-CTTTCTTCCACTACCTTATT-3' (SG-003625-02-0002). The PuroR-Cas9 expression plasmid DNA (U-005100-120) and sgRNAs were transfected into AGS cells by using jetPRIME (Polyplus transfection) for 4 h. The cells were then selected by 0.5 µg/ml puromycin for 72 h.

### Polymerase chain reaction (PCR)

The genomic DNA of RAGE-control (CRISPR-C) and RAGE-knockout (RAGE-KO) cells was extracted by using the Wizard Genomic DNA Purification Kit (Promega, Madison, WI, USA) according to the manufacturer's protocol.<sup>22</sup> The DNA was amplified by PCR with the forward primer: 5'-CTACCGAGTCCGTGTCTACC-3' and reverse primer: 5'-CACCTATGCTCACCCAGAC-3'. The program of the PCR cyclers was initially denaturation at 95 °C for 1 min, followed by 35 cycles of denaturation at 95 °C for 30 s, annealing at 65 °C for 30 s, and extension at 72 °C for 45 s. The PCR products were prepared for sequencing and analyzed by Benchling (San Francisco, CA, USA) (Fig. S3), a biotechnology platform that aligns data to reference sequences.<sup>23</sup>

## Statistical analysis

The correlation of two molecular expressions in the fluorescent image was analyzed using the Pearson correlation coefficient ( $r$ ). The statistical significance of differences between the two groups was evaluated using Student's  $t$ -test. Statistical analysis was performed by using Prism 8 (GraphPad Software).  $P < 0.05$  was considered statistically significant.

## Results

### CDT interacts with RAGE and HMGB1 to enter cells

We first investigated whether CDT interacted with RAGE. As shown in Fig. 1A, co-immunoprecipitation revealed that CDT treatment elevated CdtB binding to RAGE. To further examine whether HMGB1 plays a role in CDT delivery in the cells, cells were treated with an anti-HMGB1 antibody and found that blocking HMGB1, a reduced amount of CdtB can be transported into the cells (Fig. 1B). We then examined whether CdtB interacted with RAGE using immunofluorescence staining. Confocal microscopy showed pronounced

colocalization of RAGE (red) and CdtB (green) in the cell membrane (CTx-B, cyan), revealing an interaction between CdtB and RAGE localized within the cell membrane (Fig. 1C and D). In the CDT treatment group, a positive correlation between CdtB and RAGE localization was demonstrated through Pearson correlation coefficient analysis ( $r = 0.65$ ,  $P < 0.01$ ). These results suggest an association between CdtB and RAGE, with subsequent interactions with HMGB1 in the cell membrane.

### CDT enters the cells through the dynamin-dependent endocytosis pathway

Previous studies have shown that RAGE-mediated HMGB1 endocytosis is dynamin-dependent.<sup>24</sup> We then used dynasore, an inhibitor of dynamin GTPase activity, to examine whether dynamin inhibition interferes with CdtB delivery in cells. Endolysosomal system activation was assessed through the expression of EEA1, Rab 7, and LAMP1, which are markers of early endosomal, late endosomal, and lysosomal, respectively. As shown in Fig. 2A, CDT exposure increased the expression levels of all three markers. However, CDT-induced elevated levels of Rab7 and LAMP1 were diminished by pretreatment with dynasore. Furthermore,

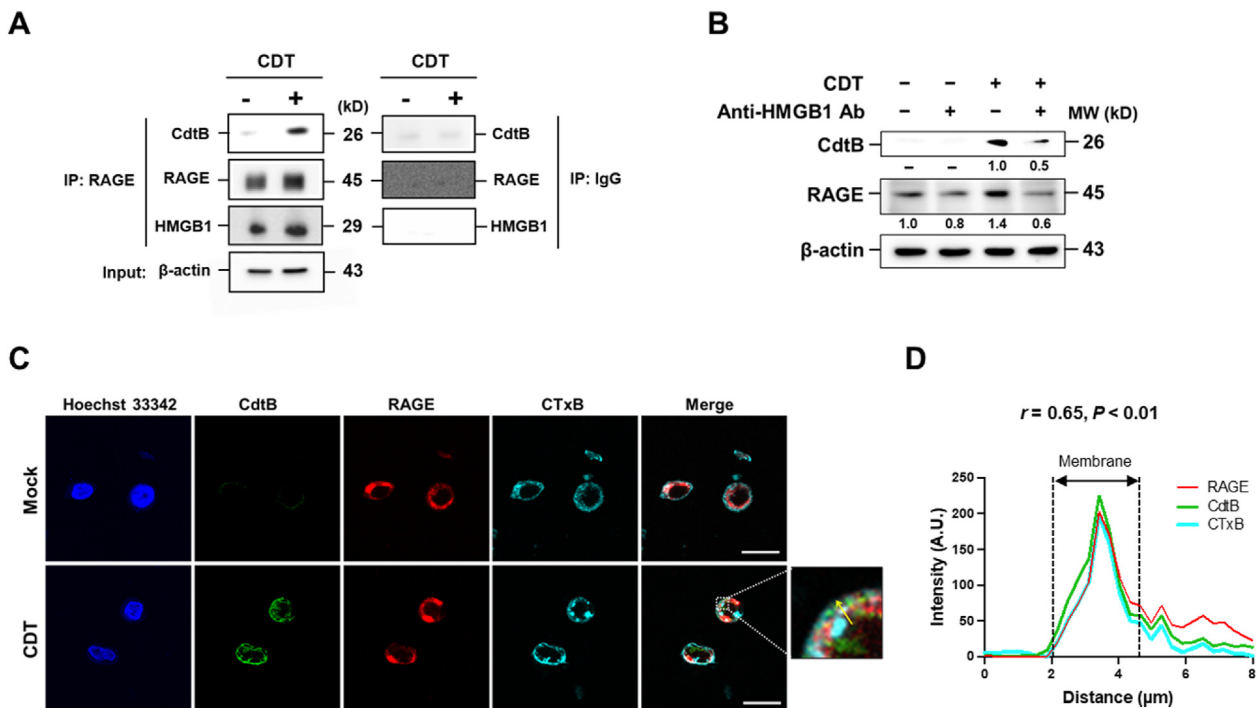


**Figure 1. Interaction of CdtB and RAGE in the cell membrane.** (A) AGS cells were treated with 100 nM CDT for 12 h. Cell lysates were treated with anti-RAGE antibody or control isotype IgG. CdtB and HMGB1 interaction with RAGE was determined using a co-immunoprecipitation assay with Western blot analysis. The expression level of  $\beta$ -actin was analyzed in total cell lysates.  $\beta$ -Actin was used as an internal control. (B) Cells were pretreated with anti-HMGB1 neutralized antibody (2  $\mu$ g/ml) for 1 h, and then exposed to CDT (100 nM) for an additional 3 h. The level of CdtB transported into cells was analyzed by western blotting. The relative protein levels were normalized to the control group and indicated below each band.  $\beta$ -Actin was used as an internal control. (C) Cells were incubated with CDT (100 nM) at 11  $^{\circ}$ C for 1 h, then incubated with anti-CdtB (green) and anti-RAGE (red) antibodies; the nuclei were stained with Hoechst 33342 (blue) and the cell membrane was probed with lipid raft marker (CTx-B) (cyan). Scale bars, 10  $\mu$ m. (D) The distribution of relative intensity of RAGE and CdtB across the cell membrane in the magnified image (right hand of panel C) was analyzed using ZEN software (Carl Zeiss). The association of CdtB and RAGE was analyzed using Pearson correlation coefficients ( $r$ ). Student's  $t$ -test processed the statistical analysis for three independent experiments.

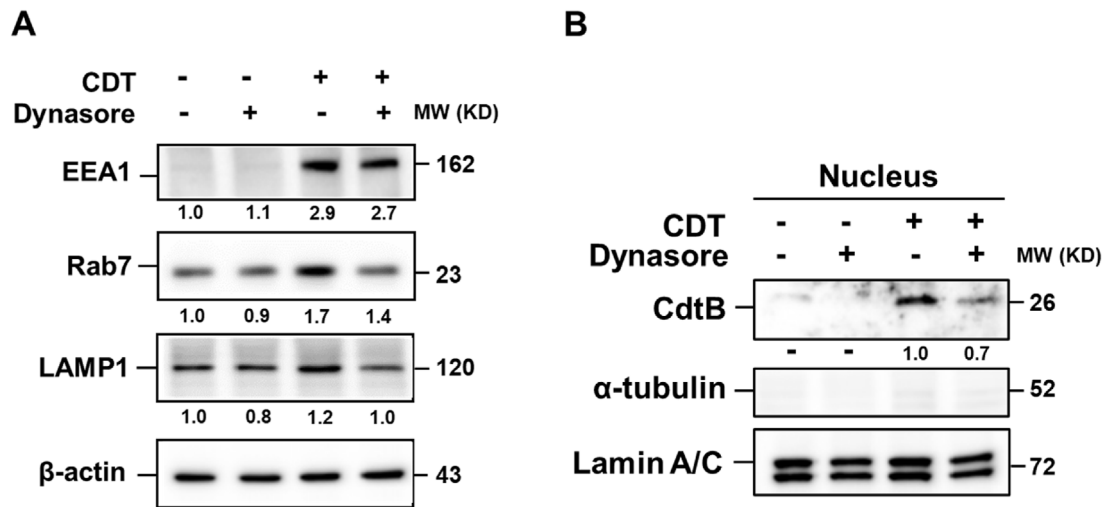


**Figure 2.** CdtB intracellular transport is mediated through dynamin-dependent endocytosis. AGS cells were pretreated with dynasore (100  $\mu$ M) for 30 min, and then exposed to CDT (100 nM) for 90 min. (A) Expression levels of EEA1, Rab 7, and LAMP1 were analyzed using western blotting. (B) Nuclear fraction was prepared for western blotting to analyze the presence of CdtB in the nucleus. The expression of  $\alpha$ -tubulin was used as a cytoplasmic marker, which was absent in the nuclear fraction. Lamin A/C was used as the nuclear loading control for nuclear extracts. The relative protein expression levels were normalized to the untreated control and indicated below each band.

dynasore treatment reduced the nuclear presence of CdtB (Fig. 2B). These results indicate that CdtB transport in cells is partially mediated through dynamin-dependent endocytosis.

### Lysosomes participate in CdtB intracellular transport

We then investigated whether lysosomes were necessary for CdtB translocation in the cytoplasm. Immunofluorescence staining showed that LAMP1 (a lysosomal marker) and CdtB colocalized in the cytoplasm (Fig. 3A and B). The fluorescence intensity of LAMP1 was significantly higher in CDT-treated cells than in mock-treated cells (Fig. 3C). Furthermore, a positive correlation between CdtB and LAMP1 localization was demonstrated through Pearson correlation coefficient analysis ( $r = 0.28$ ,  $P < 0.001$ ). We further investigated whether inhibition of lysosomal function influences CDT activity. Bafilomycin-A1 (Baf-A1), an inhibitor of vacuolar  $H^+$ -ATPase, was used to disturb endosomal acidification. As shown in Fig. 3D, Baf-A1 pretreatment significantly alleviated the CDT-induced G2/M cell cycle arrest. These results reveal that the intracellular transport of CdtB is mediated through the dynamin-dependent endocytic pathway, and lysosomes are involved in this process.

### CDT induces lysosomal rupture

As CdtB-containing endosomes fused with lysosomes, endolysosomal membranes may rupture, allowing CdtB to be released into the cytoplasm. To monitor lysosomal permeabilization, the amount of cathepsin D, a lysosomal protease, in the cytoplasm was measured. Exposure to CDT, as observed through immunofluorescence staining, resulted

in the leakage of cathepsin D into the cytoplasm (Fig. 4A and B). AGS cells were then incubated with 100 nM CDT for 1.5, 3, 6, and 9 h, and the level of cathepsin D in the cytoplasm was assessed using western blotting. As shown in Fig. 4C, the presence of cathepsin D in the cytoplasmic fraction increased upon CDT treatment from 1.5 to 6 h. These results demonstrate that CDT treatment induces lysosomal rupture, resulting in the release of cathepsin D into the cytoplasm.

### RAGE is involved in CDT-induced pathogenesis

To determine whether RAGE is essential for CDT intoxication, we generated RAGE-knockout (RAGE-KO) cells using the CRISPR/Cas9-based approach. Cells were transfected with the Cas9 expression plasmid and synthetic guide RNA, and the target site of sgRNA was deleted in RAGE knockout cells (Fig. S3). Treatment of RAGE-KO cells with CDT for 24 h arrested the cell cycle at the G2/M phase by  $52.5 \pm 4.0\%$ , which was significantly lower than that in CDT-treated CRISPR control cells (CPISPR-C) ( $63.9 \pm 5.1\%$ ) (Fig. 5). We further employed the RAGE antagonist RAP, which disrupts the interaction between RAGE and its ligands. AGS cells were pretreated with RAP for 2 h, followed by exposure to CDT for an additional 48 h, and then the cell cycle was analyzed. Our results showed that RAP significantly decreased CDT arrested cell cycle at G2/M compared to CDT treatment alone (Fig. S4). Together, these results indicate that RAGE plays an important role in CDT intoxication of cells.

### Discussion

CDT is a prominent virulence factor across numerous pathogenic Gram-negative bacteria, including *C. jejuni*,

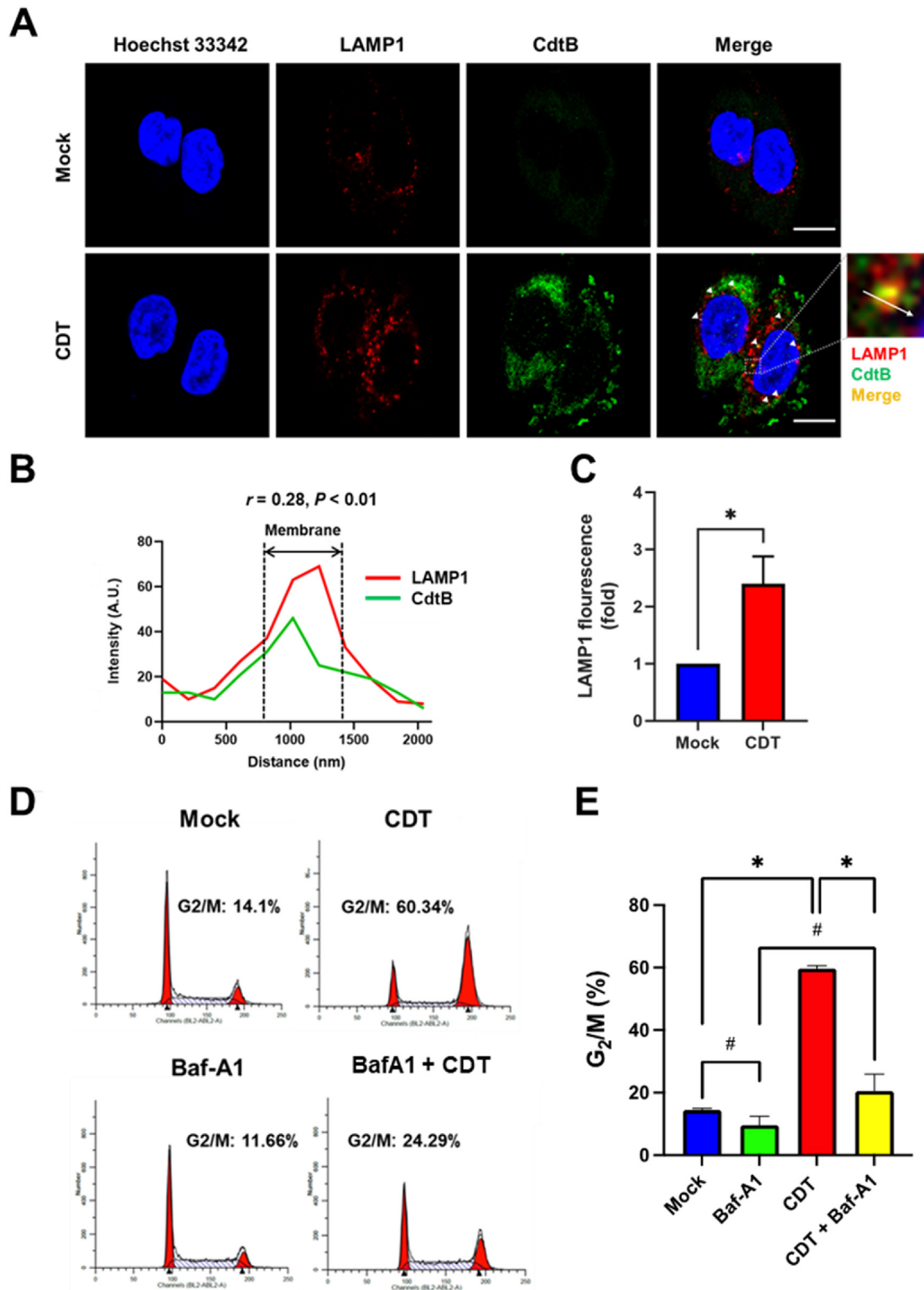


**Figure 3.** Lysosomes are involved in CdtB delivery in the cytoplasm. AGS cells were treated with CDT (100 nM) for 90 min. (A) Cells were stained with LAMP1 (red) to visualize lysosomes and stained with CdtB (green). Nuclei were probed with Hoechst 33342 (blue). The colocalization (yellow) of CdtB and LAMP1 is indicated by arrowheads. Scale bars, 10  $\mu$ m. (B) The distribution of relative intensity of LAMP1 and CdtB across the white arrow in the magnified image (right hand of panel A) was analyzed. (C) The fluorescence intensity of LAMP1 was analyzed using ZEN software (Carl Zeiss). (D) Cells were pretreated with Baf-A1 (20 nM) and then exposed to CDT (200 nM) for 24 h. Cell populations at each phase of the cell cycle were analyzed using flow cytometry. (E) The percentage of cells arrested at the G<sub>2</sub>/M phase was calculated and plotted. The data are presented as means  $\pm$  standard deviations for three independent experiments. Statistical analysis was processed by Student's *t*-test (*n* = 3). #, *p* > 0.05; \*, *P* < 0.05.

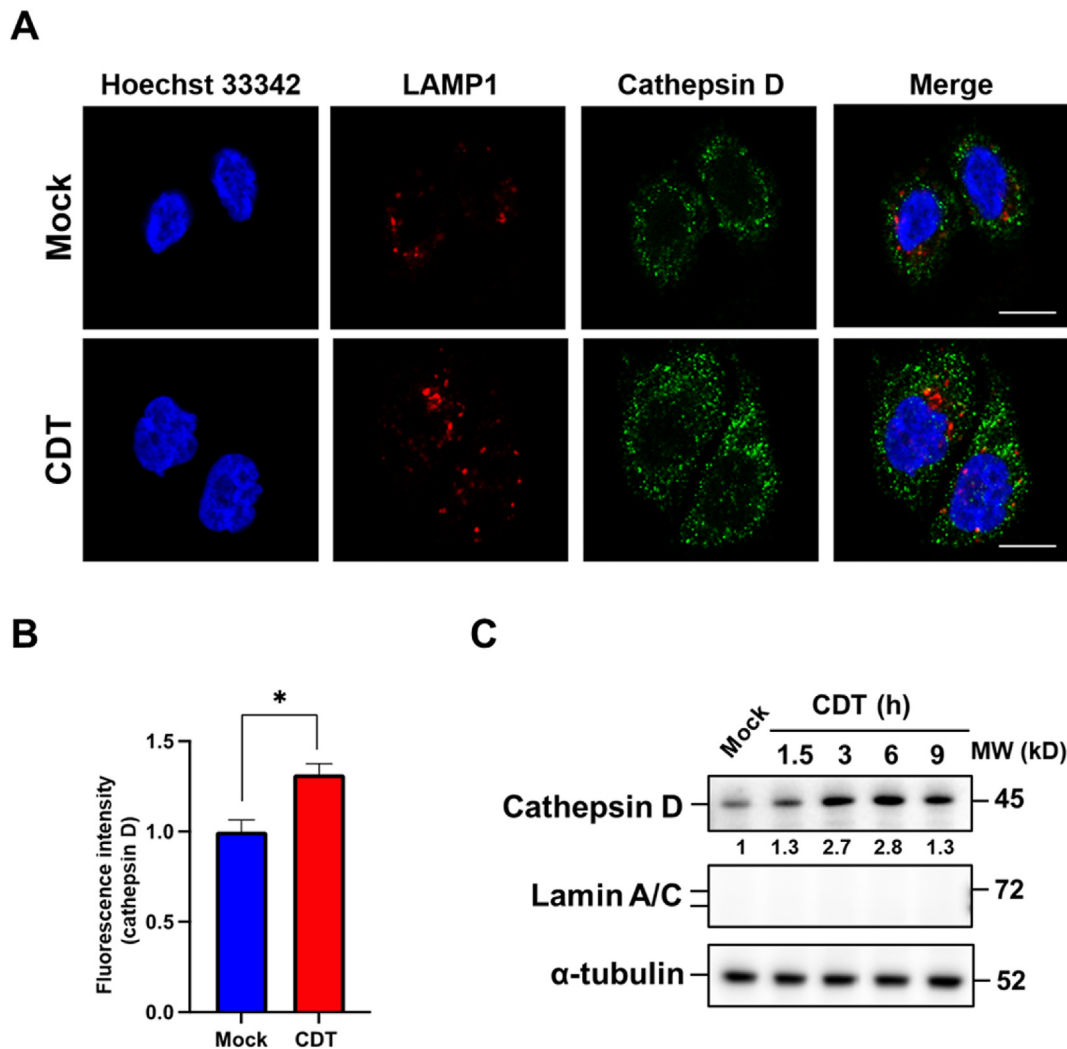


**Figure 4.** CDT promotes the release of cathepsin D in the cytoplasm. (A) AGS cells were treated with CDT (100 nM) for 3 h and stained with anti-LAMP1 (red) for visualization of lysosomes and stained with cathepsin D (green). Nuclei were probed with Hoechst 33342 (blue). Scale bars, 10  $\mu\text{m}$ . (B) The fluorescence intensity of cathepsin D was analyzed by ZEN software (Carl Zeiss). The data are presented as means  $\pm$  standard deviations for three independent experiments. Statistical analysis was calculated using Student's *t*-test ( $n = 3$ ). \*,  $P < 0.05$ . (C) AGS cells were treated with 100 nM CDT for 1.5, 3, 6, and 9 h. Cytoplasmic fraction was isolated, and the protein expression was analyzed using western blotting with antibodies against cathepsin D, Lamin A/C, and  $\alpha$ -tubulin. Lamin A/C was used to analyze the nuclear extracts and  $\alpha$ -tubulin was used as an internal control. The relative protein expression levels were normalized to the untreated control and indicated below each band.

where it contributes to effective tissue colonization, thus enhancing infectivity by subverting host defense mechanisms.<sup>25</sup> Although CDT exhibits the capability to induce cell death in a wide range of cell lineages, it has been proposed that the intoxication process of CDT may vary among different cell types.<sup>26</sup> Our recent research showed that CDT initiates DAMP-related signaling, leading to deleterious effects on target cells.<sup>16</sup> However, the mechanism underlying the intracellular transport of CDT remains elusive. The present study further provides conclusive evidence that the direct interaction between CDT, RAGE, and HMGB1 is crucial for toxin trafficking in cells. These results advance our understanding of the pertinent aspects related to CDT intoxication in host cells.

Despite the absence of definitive molecular characterization of the CDT receptor, it has been established that

cholesterol- and sphingolipid-rich lipid rafts are crucial for CDT binding to the plasma membrane. Former studies have shown that depleting cholesterol using methyl  $\beta$ -cyclodextrin reduces the ability of CDTs to associate with the surface of various cell lines, including HeLa, Jurkat, and CHO cells.<sup>27–29,10</sup> Although conflicting reports are suggesting that CDTs from different bacterial origins may bind to distinct receptors,<sup>29–31</sup> this discrepancy could be attributed to the lower degree of conservation of the binding subunits (CdtA and CdtC) among various members of this toxin family.<sup>32</sup> It is plausible that the CDT receptor could be either a glycoprotein or a glycolipid since the binding subunits adopt a ricin-like structure.<sup>33,34</sup>

Our previous research found that CDT intoxication significantly recruits RAGE into lipid rafts.<sup>16</sup> RAGE is a known PRR implicated in various diseases, including those

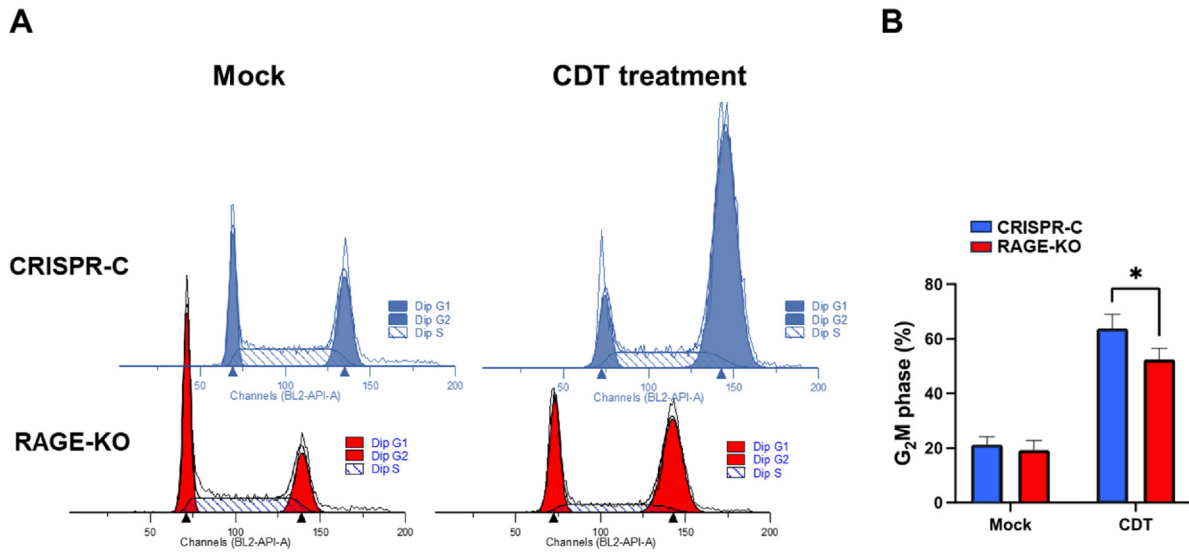


**Figure 5.** Knockout of RAGE alleviates CDT-triggered cell cycle arrest. (A) AGS cells with CRISPR-control (CRISPR-C) and RAGE-knockout (RAGE-KO) were treated with CDT (200 nM) for 24 h. The cell cycle in each stage was analyzed using flow cytometry. (B) The percentage of cell arrest at the G<sub>2</sub>/M phase was examined. The data are presented as means ± standard deviations for three independent experiments. Statistical analysis was calculated using Student’s *t*-test (*n* = 3). \*, *P* < 0.05.

caused by bacterial infections.<sup>35,36</sup> For example, RAGE-deficient mice exhibited decreased bacterial loads of *Streptococcus pneumoniae* in the lungs, spleen, and blood following infection, leading to a significantly reduced mortality rate.<sup>37</sup> Conversely, other investigations have shown that RAGE deficiency exacerbated *E. coli* infection,<sup>38</sup> and increased the mortality rate of *Klebsiella pneumoniae*

infection in mice.<sup>39</sup> These findings highlight the diverse role of RAGE in response to different bacterial infections.

Intriguingly, a recent discovery has revealed that the RAGE-HMGB1 interaction can function as a delivery system to facilitate the transport of lipopolysaccharide (LPS) into the cytoplasm, thereby causing pyroptosis.<sup>40</sup> Here, we identified RAGE as a membrane receptor for CDT, and its

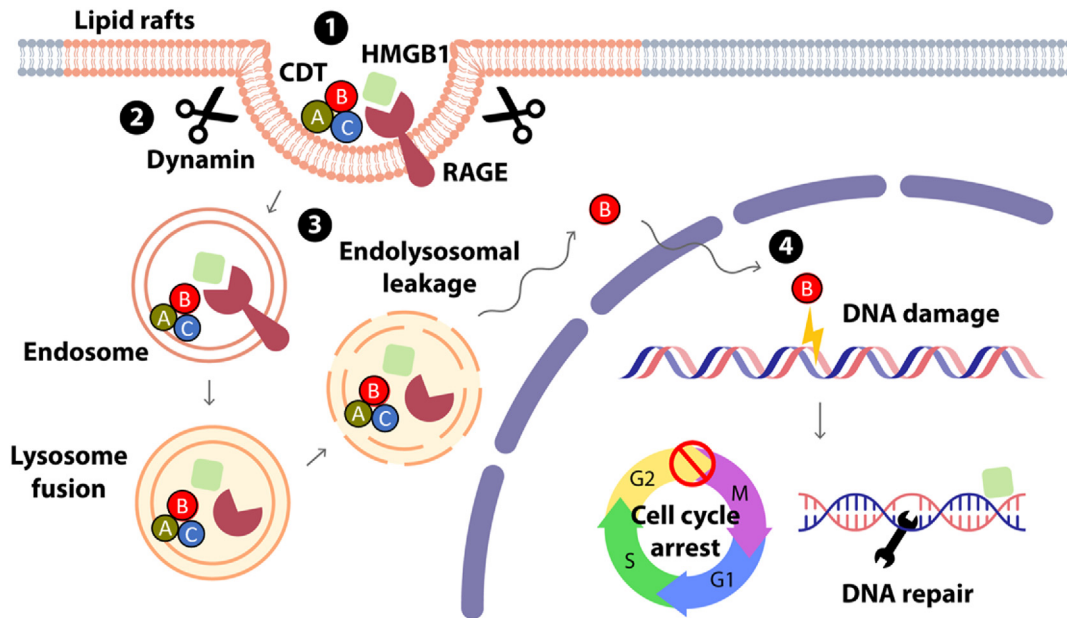


**Figure 6.** Involvement of RAGE in CdtB intracellular transport. (1) HMGB1 carries CdtB to bind with RAGE, and (2) subsequently triggers dynamin-dependent endocytosis, whereby, CDT holotoxin is sequestered in the endosome. (3) The endosome then fuses with a lysosome, forming an endolysosome, of which HMGB1 disrupts the membrane stability and allows CdtB release into the cytosol. (4) After nuclear translocation, CdtB induces DNA damage and activates DNA damage response (DDR), resulting in cell cycle arrest at the G<sub>2</sub>/M phase to permit DNA repair.



interaction with HMGB1 further facilitated CdtB delivery into cells. HMGB1 is a RAGE ligand that acts as a DAMP, participating in the induction of proinflammatory cytokine production.<sup>18</sup> *In vivo* administration of an anti-HMGB1 antibody ameliorated several bacterial infectious diseases, including carbapenem-resistant *K. pneumoniae*-induced pneumonia,<sup>41</sup> *Brucella melitensis*-associated placentitis,<sup>42</sup> and *Staphylococcus aureus*-related pneumonia.<sup>43</sup> Conditional ablation of HMGB1 in murine intestinal epithelial cells led to the development of severe *Salmonella*-related colitis,<sup>44</sup> while conditional ablation in mouse myeloid cells has increased sensitivity to endotoxin shock.<sup>45</sup> As HMGB1 serves as an autophagy regulator in the cytoplasm<sup>46,47</sup> and acts as DAMPs upon release into the extracellular environment, it is important to elucidate whether HMGB1 functions solely as a carrier during the CDT intoxication process or has other roles to play.

Following internalization, the CDT-HMGB1-RAGE complex is packaged in the endosome, which subsequently fuses with the lysosome (Fig. 6). The endolysosomal membrane is disrupted, releasing CdtB and cathepsin D into the cytoplasm. Through the analysis of Expasy, we also found that cathepsin D is capable of cleaving two positions of CdtB (data not shown). Therefore, it is interesting to investigate how CdtB simultaneously resists the acidic environment and degradative protease cathepsin D in the lysosome.

Given that CDT intoxicated a wide range of cell lineages, CDT may be able to bind to a variety of host cell receptors, each with potentially different binding affinities. Although the present study has indicated the involvement of RAGE in CDT intracellular transport, it is worth noting that the ablation of RAGE only confers partial protection against CDT toxicity. Receptors with a similar ligand-binding structure to RAGE or another unidentified molecule localized in the same membrane microdomain as RAGE may also play a role in facilitating CDT transport. Additionally, it cannot be ruled out that the receptor is cell type-specific, meaning that the structures expressed and recognized on monocytic cells or T lymphocytes may differ from those on cells of epithelial origin. Moreover, while the endolysosomal system transports CDT into the cytoplasm, the molecular mechanism of CDT nuclear localization remains to be illustrated.

## Conclusions

Consistent with our previous studies demonstrating that CDT induces an inflammatory response by increasing the expression levels of RAGE and HMGB1,<sup>16</sup> we have now shown that both RAGE and HMGB1 engage in CDT trafficking in the cells. Together, understanding the mechanism of CDT action in cells may open an opportunity to develop effective therapeutic modalities for alleviating bacterial toxin-related pathogenesis.

## Funding

This work was supported by the National Science and Technology Council, Taiwan (112-2320-B-182-036-MY3 and 112-2320-B-182-042-MY3), Chang Gung Memorial Hospital at Linkou (CMRPD1M0491-2, CORPD1M0021-3 and CMRPD1P0161-2), Research Center for Emerging Viral

Infections from the Featured Areas Research Center Program within the framework of the Higher Education Sprout Project by the Taiwan Ministry of Education, and Tomorrow Medical Foundation.

## Data availability statement

The authors confirm that the data supporting the findings of this study are available within the article.

## CRedit authorship contribution statement

**Yu-Fang Chang:** Conceptualization, Investigation, Methodology, Writing – original draft. **Yi-Ping Huang:** Data curation, Methodology, Writing – original draft. **Chia-Huei Chou:** Data curation, Methodology. **Mao-Wang Ho:** Validation, Writing – review & editing. **Hwai-Jeng Lin:** Validation, Writing – review & editing. **Chun-Ya Chen:** Data curation, Validation. **Hui-Yu Wu:** Data curation, Validation. **Yi-Ru Lai:** Methodology, Writing – original draft. **Yuan-Haw Lee:** Data curation, Methodology. **Cheng-Hsun Chiu:** Conceptualization, Supervision, Writing – review & editing. **Chih-Ho Lai:** Conceptualization, Supervision, Writing – review & editing.

## Declaration of competing interest

The authors report no conflict of interest.

## Acknowledgments

The authors would like to thank the editor and reviewers for the editorial assistance and their valuable comments. The authors sincerely thank the Microscopy Center at Chang Gung University for technical assistance.

## References

- Burnham PM, Hendrixson DR. *Campylobacter jejuni*: collective components promoting a successful enteric lifestyle. *Nat Rev Microbiol* 2018;**16**:551–65.
- Elmi A, Nasher F, Dorrell N, Wren B, Gundogdu O. Revisiting *Campylobacter jejuni* virulence and fitness factors: role in sensing, adapting, and competing. *Front Cell Infect Microbiol* 2020;**10**:607704.
- Guo YT, Hsiung CA, Wu FT, Chi H, Huang YC, Liu CC, et al. Clinical manifestations and risk factors of *Campylobacter* gastroenteritis in children in Taiwan. *Biomed J* 2023;**46**:100590.
- Liu YH, Yamazaki W, Huang YT, Liao CH, Sheng WH, Hsueh PR. Clinical and microbiological characteristics of patients with bacteremia caused by *Campylobacter* species with an emphasis on the subspecies of *C. fetus*. *J Microbiol Immunol Infect* 2019;**52**:122–31.
- He Z, Gharaibeh RZ, Newsome RC, Pope JL, Dougherty MW, Tomkovich S, et al. *Campylobacter jejuni* promotes colorectal tumorigenesis through the action of cytolethal distending toxin. *Gut* 2019;**68**:289–300.
- Omarova S, Awad K, Moos V, Püning C, Gözl G, Schulzke JD, et al. Intestinal barrier in post-*Campylobacter jejuni* irritable bowel syndrome. *Biomolecules* 2023;**13**.

7. Lara-Tejero M, Galan JE. A bacterial toxin that controls cell cycle progression as a deoxyribonuclease I-like protein. *Science* 2000;**290**:354–7.
8. Du L, Song J. Delivery, structure, and function of bacterial genotoxins. *Virulence* 2022;**13**:1199–215.
9. Pons BJ, Vignard J, Mirey G. Cytolethal distending toxin subunit B: a review of structure-function relationship. *Toxins (Basel)* 2019;**11**.
10. Lin CD, Lai CK, Lin YH, Hsieh JT, Sing YT, Chang YC, et al. Cholesterol depletion reduces entry of *Campylobacter jejuni* cytolethal distending toxin and attenuates intoxication of host cells. *Infect Immun* 2011;**79**:3563–75.
11. Frisan T. Bacterial genotoxins: the long journey to the nucleus of mammalian cells. *Biochim Biophys Acta* 2016;**1858**:567–75.
12. Lai CH, Lai CK, Lin YJ, Hung CL, Chu CH, Feng CL, et al. Characterization of putative cholesterol recognition/interaction amino acid consensus-like motif of *Campylobacter jejuni* cytolethal distending toxin C. *PLoS One* 2013;**8**:e66202.
13. Carette JE, Guimaraes CP, Wuethrich I, Blomen VA, Varadarajan M, Sun C, et al. Global gene disruption in human cells to assign genes to phenotypes by deep sequencing. *Nat Biotechnol* 2011;**29**:542–6.
14. DiRienzo JM. Uptake and processing of the cytolethal distending toxin by mammalian cells. *Toxins (Basel)* 2014;**6**:3098–116.
15. Eshraghi A, Dixon SD, Tamilselvam B, Kim EJ, Gargi A, Kulik JC, et al. Cytolethal distending toxins require components of the ER-associated degradation pathway for host cell entry. *PLoS Pathog* 2014;**10**:e1004295.
16. Lin HJ, Jiang ZP, Lo HR, Feng CL, Chen CJ, Yang CY, et al. Coalescence of RAGE in lipid rafts in response to cytolethal distending toxin-induced inflammation. *Front Immunol* 2019;**10**:109.
17. Andersson U, Yang H, Harris H. High-mobility group box 1 protein (HMGB1) operates as an alarmin outside as well as inside cells. *Semin Immunol* 2018;**38**:40–8.
18. Chen R, Kang R, Tang D. The mechanism of HMGB1 secretion and release. *Exp Mol Med* 2022;**54**:91–102.
19. Gao S, Wake H, Sakaguchi M, Wang D, Takahashi Y, Teshigawara K, et al. Histidine-rich glycoprotein inhibits high-mobility group box-1-mediated pathways in vascular endothelial cells through CLEC-1A. *iScience* 2020;**23**:101180.
20. Sims GP, Rowe DC, Rietdijk ST, Herbst R, Coyle AJ. HMGB1 and RAGE in inflammation and cancer. *Annu Rev Immunol* 2010;**28**:367–88.
21. Bui NN, Li CY, Wang LY, Chen YA, Kao WH, Chou LF, et al. *Clostridium scindens* metabolites trigger prostate cancer progression through androgen receptor signaling. *J Microbiol Immunol Infect* 2023;**56**:246–56.
22. Kuo CJ, Ke JN, Kuo T, Lin CY, Hsieh SY, Chiu YF, et al. Multiple amino acid substitutions in penicillin-binding protein-1A confer amoxicillin resistance in refractory *Helicobacter pylori* infection. *J Microbiol Immunol Infect* 2023;**56**:40–7.
23. O’Leary NA, Wright MW, Brister JR, Ciufo S, Haddad D, McVeigh R, et al. Reference sequence (RefSeq) database at NCBI: current status, taxonomic expansion, and functional annotation. *Nucleic Acids Res* 2016;**44**:D733–45.
24. Xu J, Jiang Y, Wang J, Shi X, Liu Q, Liu Z, et al. Macrophage endocytosis of high-mobility group box 1 triggers pyroptosis. *Cell Death Differ* 2014;**21**:1229–39.
25. Scuron MD, Boesze-Battaglia K, Dlakic M, Shenker BJ. The cytolethal distending toxin contributes to microbial virulence and disease pathogenesis by acting as a tri-perditious toxin. *Front Cell Infect Microbiol* 2016;**6**:168.
26. Fais T, Delmas J, Serres A, Bonnet R, Dalmaso G. Impact of CDT toxin on human diseases. *Toxins (Basel)* 2016;**8**.
27. Boesze-Battaglia K, Besack D, McKay T, Zekavat A, Otis L, Jordan-Sciutto K, et al. Cholesterol-rich membrane microdomains mediate cell cycle arrest induced by *Actinobacillus actinomycetemcomitans* cytolethal-distending toxin. *Cell Microbiol* 2006;**8**:823–36.
28. Boesze-Battaglia K, Dhingra A, Walker LM, Zekavat A, Shenker BJ. Internalization and intoxication of human macrophages by the active subunit of the *Aggregatibacter actinomycetemcomitans* cytolethal distending toxin is dependent upon cellugryrin (Synaptogryrin-2). *Front Immunol* 2020;**11**:1262.
29. Eshraghi A, Maldonado-Arocho FJ, Gargi A, Cardwell MM, Prouty MG, Blanke SR, et al. Cytolethal distending toxin family members are differentially affected by alterations in host glycans and membrane cholesterol. *J Biol Chem* 2010;**285**:18199–207.
30. McSweeney LA, Dreyfus LA. Carbohydrate-binding specificity of the *Escherichia coli* cytolethal distending toxin CdtA-II and CdtC-II subunits. *Infect Immun* 2005;**73**:2051–60.
31. Mise K, Akifusa S, Watarai S, Ansai T, Nishihara T, Takehara T. Involvement of ganglioside GM3 in G(2)/M cell cycle arrest of human monocytic cells induced by *Actinobacillus actinomycetemcomitans* cytolethal distending toxin. *Infect Immun* 2005;**73**:4846–52.
32. Hu X, Nestic D, Stebbins CE. Comparative structure-function analysis of cytolethal distending toxins. *Proteins* 2006;**62**:421–34.
33. Nestic D, Hsu Y, Stebbins CE. Assembly and function of a bacterial genotoxin. *Nature* 2004;**429**:429–33.
34. Sandvig K, Grimmer S, Iversen TG, Rodal K, Torgersen ML, Nicoziani P, et al. Ricin transport into cells: studies of endocytosis and intracellular transport. *Int J Med Microbiol* 2000;**290**:415–20.
35. Giridharan VV, Generoso JS, Collodel A, Domingui D, Faller CJ, Tardin F, et al. Receptor for advanced glycation end products (RAGE) mediates cognitive impairment triggered by pneumococcal meningitis. *Neurotherapeutics* 2021;**18**:640–53.
36. Miyashita D, Inoue R, Tsuno T, Okuyama T, Kyohara M, Nakahashi-Oda C, et al. Protective effects of S100A8 on sepsis mortality: links to sepsis risk in obesity and diabetes. *iScience* 2022;**25**:105662.
37. van Zoelen MA, Schouten M, de Vos AF, Florquin S, Meijers JC, Nawroth PP, et al. The receptor for advanced glycation end products impairs host defense in pneumococcal pneumonia. *J Immunol* 2009;**182**:4349–56.
38. van Zoelen MA, Schmidt AM, Florquin S, Meijers JC, de Beer R, de Vos AF, et al. Receptor for advanced glycation end products facilitates host defense during *Escherichia coli*-induced abdominal sepsis in mice. *J Infect Dis* 2009;**200**:765–73.
39. Achouiti A, de Vos AF, van ’t Veer C, Florquin S, Tanck MW, Nawroth PP, et al. Receptor for advanced glycation end products (RAGE) serves a protective role during *Klebsiella pneumoniae*-induced pneumonia. *PLoS One* 2016;**11**:e0141000.
40. Deng M, Tang Y, Li W, Wang X, Zhang R, Zhang X, et al. The endotoxin delivery protein HMGB1 mediates caspase-11-dependent lethality in sepsis. *Immunity* 2018;**49**:740–753 e7.
41. Liming S, Guixia L, Wenxin S, Guirong T. HMGB1 signaling blocking protects against carbapenem-resistant *klebsiella pneumoniae* in a murine model of infection. *Exp Lung Res* 2018;**44**:263–71.

42. Liu X, Zhou M, Wu J, Wang J, Peng Q. HMGB1 release from trophoblasts contributes to inflammation during *Brucella melitensis* infection. *Cell Microbiol* 2019;21:e13080.
43. Fink MP. HMGB1 as a drug target in staphylococcal pneumonia. *Crit Care* 2014;18:131.
44. Zhang YG, Zhu X, Lu R, Messer JS, Xia Y, Chang EB, et al. Intestinal epithelial HMGB1 inhibits bacterial infection via STAT3 regulation of autophagy. *Autophagy* 2019;15:1935–53.
45. Yanai H, Matsuda A, An J, Koshiba R, Nishio J, Negishi H, et al. Conditional ablation of HMGB1 in mice reveals its protective function against endotoxemia and bacterial infection. *Proc Natl Acad Sci U S A* 2013;110:20699–704.
46. Shang J, Zhao F, Cao Y, Ping F, Wang W, Li Y. HMGB1 mediates lipopolysaccharide-induced macrophage autophagy and pyroptosis. *BMC Mol Cell Biol* 2023;24:2.
47. Tang D, Kang R, Livesey KM, Cheh CW, Farkas A, Loughran P, et al. Endogenous HMGB1 regulates autophagy. *J Cell Biol* 2010;190:881–92.

## Appendix A. Supplementary data

Supplementary data to this article can be found online at <https://doi.org/10.1016/j.jmii.2024.07.007>.